Inorganic Chemistry
Article

Inorg. Chem. **2010**, *49*, 675–685 **675**
DOI: 10.1021/ic901972h

Tripodal 4-Pyridyl-Derived Host Ligands and Their Metallo-Supramolecular Chemistry: Stella Octangula and Bowl-Shaped Assemblies

Tanya K. Ronson,[†] Christopher Carruthers,[†] Julie Fisher,[†] Thierry Brotin,[‡] Lindsay P. Harding,[§] Pierre J. Rizkallah,[∥] and Michaele J. Hardie*[,†]

[†]*School of Chemistry, University of Leeds, Woodhouse Lane, Leeds, LS2 9JT, United Kingdom,* [‡]*Stéréochimie et Interactions Moléculaires, UMR 5532 CNRS/ENS-Lyon, 46 Allée d'Italie, 69364 Lyon 07, France,* [§]*Department of Chemical and Biological Sciences, University of Huddersfield, Huddersfield, HD1 3DH, United Kingdom, and* [∥]*STFC Daresbury Laboratory, Daresbury, Warrington, WA4 4AD, United Kingdom*

Received October 6, 2009

The synthesis of five new cyclotriveratrylene derivatives with 4-pyridyl side arms is reported, along with the crystal structures of three of these. Three ligands with extended 4-pyridylphenyl side arms and a ligand derived from cyclotriphenolene have been shown to form $[Pd_6L_8]^{12+}$ stella octangula assemblies using diffusion-ordered spectroscopy NMR and electrospray MS techniques. This confirms the generality of the stella octagula assembly, providing that the ligand arms show a degree of rigidity. The more flexible ether-linked ligand tris(4-pyridylmethyl)cyclotriguaiacylene forms a smaller $[Pd_3L_4]^{6+}$ bowl-shaped assembly in the solid state and in solution. The previously reported ligand tris(4-pyridylmethylamino)cyclotriguaiacylene forms a similar assembly in solution.

Introduction

Cyclotriveratrylene (CTV) is a molecular host with a relatively rigid shallow bowl-shaped cavity.[1] Recent interest in CTV chemistry includes applications in liquid crystals,[2] gas-binding,[3] organometallic cryptophanes,[4] organo-gels,[5] metallo-gels,[6] anion sensing,[7] fullerene separations,[8] metallo-supramolecular assemblies,[9−15] and coordination polymers.[16] Both CTV and its chiral analogs cyclotriguaiacylene (CTG) and tris-amino cyclotriguaiacylene (aCTG) can be converted into extended-arm host molecules through functionalization at the upper rim.[17]

The self-assembly of 3D metallo-supramolecular species from transition metals ions and multifunctional ligands is well established, and a huge range of polyhedral/prismatic

*To whom correspondence should be addressed. E-mail: m.j.hardie@leeds.ac.uk.

(1) For a review, see: Collet, A. *Tetrahedron* **1987**, *43*, 5725–5759.
(2) (a) Rio, Y.; Nierengarten, J.-F. *Tetrahedron Lett*. **2002**, *43*, 4321–4324. (b) Felder, D.; Heinrich, B.; Guillon, D.; Nicoud, J.-F.; Nierengarten, J.-F. *Chem.—Eur. J*. **2000**, *6*, 3501–3507.
(3) Fogarty, H. A.; Berthault, P.; Brotin, T.; Huber, G.; Desvaux, H.; Dutasta, J.-P. *J. Am. Chem. Soc*. **2007**, *129*, 10332–10333.
(4) Fairchild, R. M.; Holman, K. T. *J. Am. Chem. Soc*. **2005**, *127*, 16364–16365.
(5) Bardelang, D.; Camerel, F.; Ziessel, R.; Schmutz, M.; Hannon, M. J. *J. Mater. Chem*. **2008**, *18*, 489–494.
(6) Westcott, A.; Sumby, C. J.; Walshaw, R. D.; Hardie, M. J. *New J. Chem*. **2009**, *33*, 902–912.
(7) (a) Zhang, S.; Echegoyen, L. *J. Am. Chem. Soc*. **2005**, *127*, 2006–2011. (b) Gawenis, J. A.; Holman, T. K.; Atwood, J. L.; Jurisson, S. S. *Inorg. Chem*. **2002**, *41*, 6028–6031.
(8) Huerta, E.; Cequier, E.; de Mendoza, J. *Chem. Commun*. **2007**, 5016–5018.
(9) Sumby, C. J.; Fisher, J.; Prior, T. J.; Hardie, M. J. *Chem.—Eur. J*. **2006**, *12*, 2945–2959.
(10) Sumby, C. J.; Hardie, M. J. *Angew. Chem., Int. Ed*. **2005**, *44*, 6395–6399.
(11) Sumby, C. J.; Carr, M. J.; Franken, A.; Kennedy, J. D.; Kilner, C. A.; Hardie, M. J. *New J. Chem*. **2006**, *30*, 1390–1396.
(12) Ronson, T. K.; Fisher, J.; Harding, L. P.; Hardie, M. J. *Angew. Chem., Int. Ed*. **2007**, *46*, 9086–9088.
(13) Westcott, A.; Fisher, J.; Harding, L. P.; Rizkallah, P.; Hardie, M. J. *J. Am. Chem. Soc*. **2008**, *130*, 2950–2951.
(14) Ronson, T. K.; Fisher, J.; Harding, L. P.; Rizkallah, P. J.; Warren, J. E.; Hardie, M. J. *Nature Chem*. **2009**, *1*, 212–216.
(15) Zhong, Z.; Ikeda, A.; Shinkai, S.; Sakamoto, S.; Yamaguchi, K. *Org. Lett*. **2001**, *3*, 1085–1087.
(16) (a) Sumby, C. J.; Hardie, M. J. *Cryst. Growth Des*. **2005**, *5*, 1321–1324. (b) Hardie, M. J.; Sumby, C. J. *Inorg. Chem*. **2004**, *43*, 6872–6874. (c) Ronson, T. K.; Hardie, M. J. *CrystEngComm* **2008**, *10*, 1731–1734. (d) Mough, S. T.; Holman, K. T. *Chem. Commun*. **2008**, 1407–1409.
(17) Hardie, M. J.; Sumby, C. J.; Mills, R. M. *Org. Biomol. Chem*. **2004**, *2*, 2958–2964.
(18) For some recent examples and some reviews, see: (a) He, Q.-T.; Li, X.-P.; Liu, Y.; Yu, Z.-Q.; Wang, W.; Su, C.-Y. *Angew. Chem., Int. Ed*. **2009**, *48*, 6156–6159. (b) Duriska, M. B.; Neville, S. M.; Moubaraki, B.; Cashion, J. D.; Halder, G. J.; Chapman, K. W.; Balde, C.; Létard, J.-F.; Murray, K. S.; Kepert, C. J.; Batten, S. R. *Angew. Chem., Int. Ed*. **2009**, *48*, 2549–2552. (c) Lu, Z.; Knobler, C. B.; Furukawa, H.; Wang, B.; Liu, G.; Yaghi, O. M. *J. Am. Chem. Soc*. **2009**, *131*, 12532–12533. (d) Ghosh, K.; Hu, J.; White, H. S.; Stang, P. J. *J. Am. Chem. Soc*. **2009**, *131*, 6695–6697. (e) Ghosh, K.; Mukherjee, P. S. *Organometallics* **2008**, *27*, 316–319. (f) Oppel, I. M.; Foecker, K. *Angew. Chem., Int. Ed*. **2008**, *47*, 402–405. (g) Ward, M. D. *Chem. Commun*. **2009**, 4487–4499. (h) Seidel, S. R.; Stang, P. J. *Acc. Chem. Res*. **2002**, *35*, 972–983. (i) Fujita, M.; Umemoto, K.; Yoshizawa, M.; Fujita, N.; Kusukawa, T.; Biradha, K. *Chem. Commun*. **2001**, 509–518. (j) Sweigers, G. F.; Malefeste, T. J. *Chem. Rev*. **2000**, *100*, 3483–3537. (k) Caulder, D. L.; Raymond, K. N. *Acc. Chem. Res*. **1999**, *32*, 975–982.

Published on Web 12/14/2009

Scheme 1. Self-Assembly of Stella Octangula $[Pd_6(\mathbf{1})_8]^{12+}$ Cage with Detail from Crystal Structure (Box)[12]

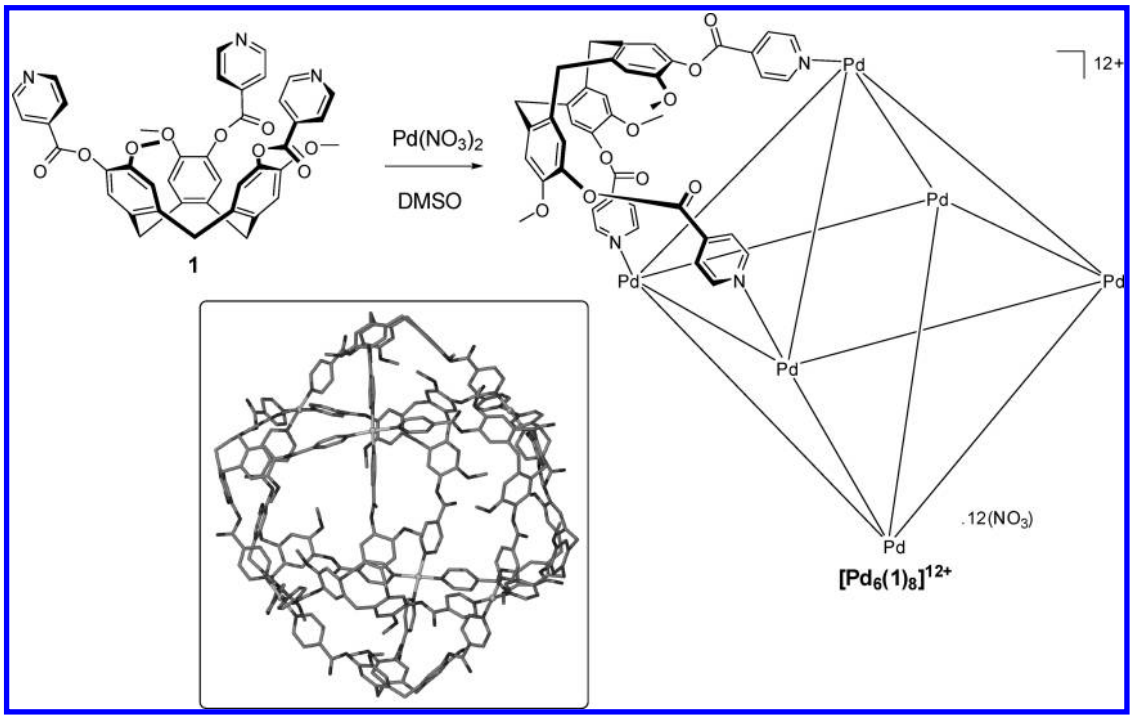

structures have been reported.[18−23] The majority of such polyhedra utilize planar or linear ligands with a much smaller number involving cavitand ligands. Many of these involve dimeric capsule assemblies,[19] with only rare examples of higher assemblies with cavitand ligands known.[20] Metal-based assemblies incorporating 3-fold symmetric cyclotriveratrylene ligands are particularly unusual. The bowl shape of a CTV derivative provides a convergent binding mode, and such ligands can form assemblies with greater internal volumes than would a corresponding planar analog and give the resulting assemblies a stellated aspect. Furthermore, the CTV-type ligands impart embedded molecular recognition sites within the assemblies, and it has been shown that simple host−guest interactions at these sites can have a directing influence on the overall self-assembly process.[9] Shinkai and co-workers have reported $[M_3L_2]$ capsules involving CTV-type ligands.[15] We have reported $[Ag_2L_2]^{2+}$ capsules,[9,10] $[Ag_4L_4]^{4+}$ "star-burst" tetrahedra[9−11] as well as a $[Ag_4L_4]^{4+}$ self-included tetrahedra,[21] a $[M_3L_2]_2$ [2]catenane,[13] and a topologically nontrivial $[Pd_4L_4]^{8+}$ "Solomon's cube".[14]

We have also recently reported a $[Pd_6L_8]^{12+}$ metallo-supramolecular assembly with a stella octangula structure which forms from the reaction of tris(isonicotinoyl)cyclotriguaiacylene (**1**) with $Pd(NO_3)_2$ in dimethylsulfoxide (DMSO), Scheme 1.[12] Square planar Pd(II) with highly labile ligands such as NO_3^- has been combined with multifunctional ligands to give a number of 3D metallo-supramolecular assemblies.[22] The $[Pd_6L_8]^{12+}$ stella octangula features Pd(II) cations in an octahedral arrangement and a ligand, **1**, occupying each face of the octahedron. A stella octangula is the first stellation of an octahedron, which is where the edges of the octahedron are extended until they meet at a point, resulting in a polyhedron with a spiked appearance. The pyramidal shape of **1** means that $[Pd_6L_8]^{12+}$ has the appearance of a stella octangula. M_6L_8 metallo-supramolecular assemblies have also been reported by several other groups.[23]

Having the binding pyridyl groups in the 4 position in ligand **1** is an important aspect of the design of the stella octangula, and we report herein our investigations into whether other CTG-based or aCTG-based ligands with pyridyl binding sites in a 4 disposition form analogous $[Pd_6L_8]^{12+}$ stella octangula cages. The cage complex $[Pd_6(\mathbf{1})_8]^{12+}$ has a significant internal volume as well as

(19) For examples, see: (a) Gruppi, F.; Boccini, F.; Elviri, L.; Dalcanale, E. *Tetrahedron* **2009**, *65*, 7289–7295. (b) Power, N. P.; Dalgarno, S. J.; Atwood, J. L. *New J. Chem.* **2007**, *31*, 17–20. (c) Haino, T.; Kobayashi, M.; Chikaraishi, M.; Fukazawa, Y. *Chem. Commun.* **2005**, 2321–2323. (d) Kobayashi, K.; Yamada, Y.; Yamanaka, M.; Sei, Y.; Yamaguchi, K. *J. Am. Chem. Soc.* **2004**, *126*, 13896–13897. (e) Pirondi, L.; Bertolini, F.; Cantadori, B.; Ugozzoli, F.; Massera, C.; Dalcanale, E. *Proc. Natl. Acad. Sci. U. S. A.* **2002**, *99*, 4911–4915.

(20) (a) McKinlay, R. M.; Thallapally, P. K.; Atwood, J. L. *Chem. Commun.* **2006**, 2956–2958. (b) McKinlay, R. M.; Cave, G. W. V.; Atwood, J. L. *Proc. Natl. Acad. Sci. U. S. A.* **2005**, *102*, 5944–5948. (c) McKinlay, R. M.; Thallapally, P. K.; Cave, G. W. V.; Atwood, J. L. *Angew. Chem., Int. Ed.* **2005**, *44*, 5733–5736. (d) Fox, O. D.; Drew, M. G. B.; Beer, P. D. *Angew. Chem., Int. Ed.* **2000**, *39*, 135–140. (e) Fox, O. D.; Drew, M. G. B.; Wilkinson, E. J. S.; Beer, P. D. *Chem. Commun.* **2000**, 391–392.

(21) Carruthers, C.; Ronson, T. K.; Sumby, C. J.; Westcott, A.; Harding, L. P.; Prior, T. J.; Rizkallah, P.; Hardie, M. J. *Chem.—Eur. J.* **2008**, *14*, 10286–10296.

(22) For examples, see: (a) Chand, D. K.; Biradha, K.; Kawano, M.; Sakamoto, S.; Yamaguchi, K.; Fujita, M. *Chem. As. J.* **2006**, *1*, 82–90. (b) Sato, S.; Iida, J.; Suzuki, K.; Kawano, M.; Ozeki, T.; Fujita, M. *Science* **2006**, *313*, 1273–1276. (c) Suzuki, K.; Tominaga, M.; Kawano, M.; Fujita, M. *Chem Comm.* **2009**, 1638–1640. (d) Suzuki, K.; Kawano, M.; Fujita, M. *Angew. Chem., Int. Ed.* **2007**, *46*, 2819–2822. (e) Tominaga, M.; Suzuki, K.; Kawano, M.; Kusukawa, T.; Ozeki, T.; Sakamoto, S.; Yamaguchi, K.; Fujita, M. *Angew. Chem., Int. Ed.* **2004**, *43*, 5621–5625.

(23) (a) Chand, D. K.; Biradha, K.; Fujita, M.; Sakamoto, S.; Yamaguchi, K. *Chem. Commun.* **2002**, 2486–2487. (b) Chand, D. K.; Fujita, M.; Biradha, K.; Sakamoto, S.; Yamaguchi, K. *Dalton Trans.* **2003**, 2750–2756. (c) Moon, D.; Kang, S.; Park, J.; Lee, K.; John, R. P.; Won, H.; Seong, G. H.; Kim, Y. S.; Kim, G. H.; Rhee, H.; Lah, M. S. *J. Am. Chem. Soc.* **2006**, *128*, 3530–3531. (d) Liu, H.-K.; Tong, X. *Chem. Commun.* **2002**, 1316–1317. (e) Ghosh, S.; Mukherjee, P. S. *J. Org. Chem.* **2006**, *71*, 8412–8416. (f) Hiraoka, S.; Harano, K.; Shiro, M.; Ozawa, Y.; Yasuda, N.; Toriumi, K.; Shionoya, M. *Angew. Chem., Int. Ed.* **2006**, *45*, 6488–6491.

Scheme 2. Synthetic Routes to New Ligands

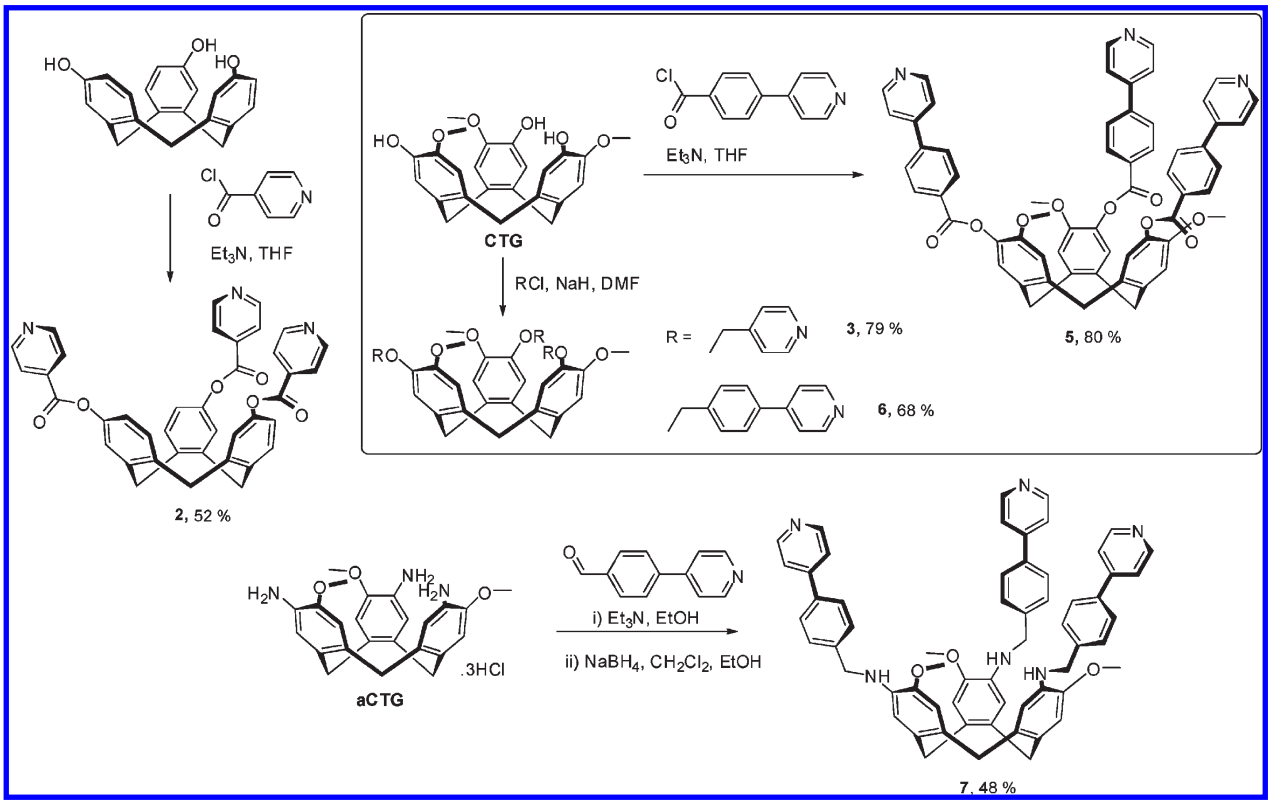

internal binding sites, which gives it the potential to act as a nanoscale vessel. The surface of $[Pd_6(\mathbf{1})_8]^{12+}$ is not fully enclosed and has eight windows of ca. 7 × 9 Å dimensions, although access through these windows is partially blocked by methoxy groups of the ligand. The series of ligands with 4-pyridyl donor groups, **2**−**7**, was designed in order to test the generality of the stella octangula cage formation and to manipulate both the size of the overall assembly and these windows on its surface.

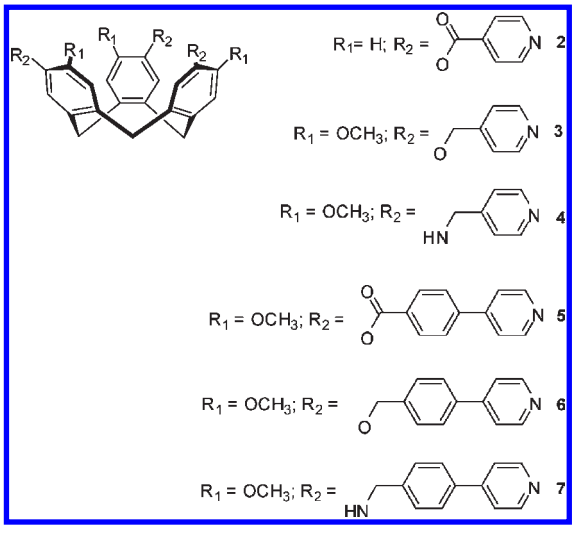

The ligand tris(isonicotinoyl)cyclotriphenolene **2** is directly analogous to **1** but based on a cyclotriphenolene core without the OMe goups at the rim. It therefore has the potential to form a cage with larger windows than were seen for $[Pd_6(\mathbf{1})_8]^{12+}$. Ligands investigated of the same size as **1** but with more flexible linker groups between the CTG core and 4-pyridyl groups were tris(4-pyridylmethyl)cyclotriguaiacylene, **3**, and the previously reported tris(4-pyridylmethylamino)-cyclotriguaiacylene, **4**.[9] Ligands tris{4-(4-pyridyl)phenylester}-cyclotriguaiacylene, **5**; tris{4-(4-pyridyl)benzyl}cyclotriguaiacylene, **6**; and tris{4-(4-pyridyl)benzyl-amino}cyclotriguaiacylene, **7**, all feature longer 4-(4-pyridyl)phenyl "arms" extending from the host core. With the majority of ligands investigated, $[Pd_6L_8]^{12+}$ cages were indeed formed, although an alternative $[Pd_3L_4]^{6+}$ open bowl-shaped assembly was found with two of the more flexible ligands.

Results and Discussion

Ligand Synthesis and Structures. The synthetic routes to previously unreported ligands are summarized in Scheme 2. All ligands were isolated as racemic mixtures in moderate to good yields. Tris(isonicotinoyl)cyclotriphenolene (**2**) was prepared by the reaction of cyclotriphenolene[24] with isonicotinoyl chloride hydrochloride in THF, in the presence of a base. Similarly, tris{4-(4-pyridyl)phenylester}cyclotriguaiacylene (**5**) was prepared by the reaction of 4-(4-pyridyl)benzoyl chloride hydrochloride with cyclotriguaiacylene (CTG)[25] in the presence of a base. The ether linked derivatives tris(4-pyridylmethyl)cyclotriguaiacylene (**3**) and tris{4-(4-pyridyl)-benzyl}cyclotriguaiacylene (**6**) were prepared by the reaction of CTG with 4-bromomethylpyridine or 4-[4-(chloromethyl)phenyl]pyridine hydrochloride, repectively,

(24) Brotin, T.; Roy, V.; Dutasta, J.-P. *J. Org. Chem.* **2005**, *70*, 6187–6195.
(25) Brotin, T.; Devic, T.; Lesage, A.; Emsley, L.; Collet, A. *Chem.—Eur. J.* **2001**, *7*, 1561–1573.

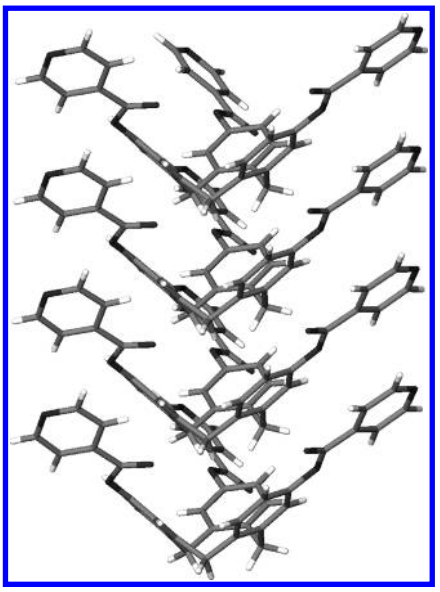

Figure 1. Section of an aligned infinite column from the crystal structure of **2**.

in dry dimethylformamide (DMF) with NaH as a base. Tris{4-(4-pyridyl)benzyl-amino}cyclotriguaiacylene (**7**) was synthesized in two steps from the precursor 3,8,13-triamino-2,7,12-trimethoxy-10,15-dihydro-5*H*-tribenzo[*a*,*d*,*g*]cyclononene (aCTG),[26] with initial formation of the imine through reaction with 4-(4-pyridyl)benzaldehyde followed by reduction with sodium borohydride. All ligands were characterized by NMR, IR, mass spectrometry, and elemental analysis. Single crystals were obtained of **2** and **3** (in two phases) and of a solvate of **5**, and their X-ray structures are briefly described below.

Ligand **2** crystallizes in space group $P\bar{1}$ with one complete molecule in the asymmetric unit. The three pyridyl arms are directed outward, forming an extended cavity which acts as a host for another molecule of **2**, resulting in aligned infinite stacks of the ligand, Figure 1. The long centroid−centroid distances of 4.679 Å between the aromatic rings of adjacent ligands preclude any $\pi-\pi$ interactions.

Two phases of **3** were obtained from different crystallization solvents. Phase **3a** was isolated by vapor diffusion of diisopropyl ether into a $CDCl_3$ solution of **3**, while phase **3b** was obtained from vapor diffusion of diethyl ether into an acetonitrile solution. Neither crystal structure showed any appreciable inclusion of a solvent, as indicated by low residual electron density from the crystal structure refinements. With **3a**, ligand **3** crystallizes in the monoclinic cell with one molecule of **3** in the asymmetric unit, Figure 2a. An offset infinite stack of ligands is formed with one OMe group of each ligand being directed into the molecular cavity of another, Figure 2a. A face-to-face $\pi-\pi$ stacking interaction occurs between a pyridyl ring of one ligand and one of the aromatic rings of the CTV core at a ring centroid separation of 3.736 Å. Phase **3b** crystallizes in the rhombohedral space group $R\bar{3}$, with two molecules of **3** in the asymmetric unit, Figure 2b. Phase **3b** also shows offset infinite stacks of ligands,

(26) Garcia, C.; Malthête, J.; Collet, A. *Bull. Soc. Chim. Fr.* **1993**, *130*, 93–95.

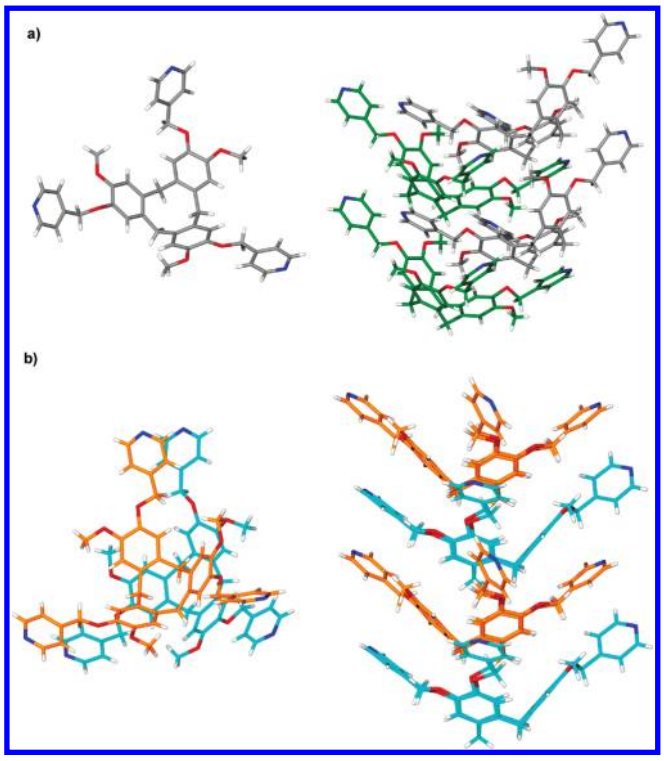

Figure 2. From the crystal structures of (a) **3a** and (b) **3b**. The asymmetric units are shown of the left and misaligned columns of ligand **3** on the right with crystallographically equivalent molecules shown in the same colors.

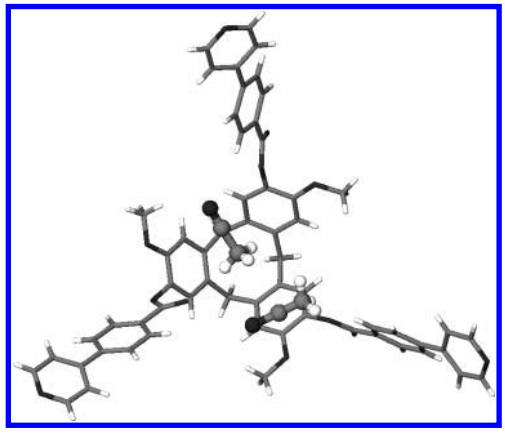

Figure 3. Detail from the crystal structure of $\mathbf{5}\cdot 3^{1}/_{3}MeCN\cdot {}^{1}/_{3}H_2O$ showing host−guest interactions between **5** and CH_3CN.

although this occurs in a distinct manner to that of **3a**, and an OMe group of one ligand is not directed into the bowl of an adjacent ligand as for **3b**, Figure 2b. Infinite stacks of ligand **3** within **3b** pack together in a manner that creates small circular channels approximately 10 Å in diameter.

Slow evaporation of a solution of **5** in acetonitrile gave colorless crystals of $\mathbf{5}\cdot 3^{1}/_{3}MeCN\cdot {}^{1}/_{3}H_2O$ which crystallize in the trigonal space group *P*31*c*. The asymmetric unit contains one molecule of **5**, three acetonitrile solvate molecules, and a further acetonitrile and water solvate molecules located on special positions with fractional occupancy. Each molecule of **5** is a host for an acetonitrile molecule (Figure 3), with the hydrophobic end of the

Scheme 3. Schematic Giving a Summary of the Formation of Stella Octangula or Open-Bowl Assemblies with the Different Ligands **1**−**7**

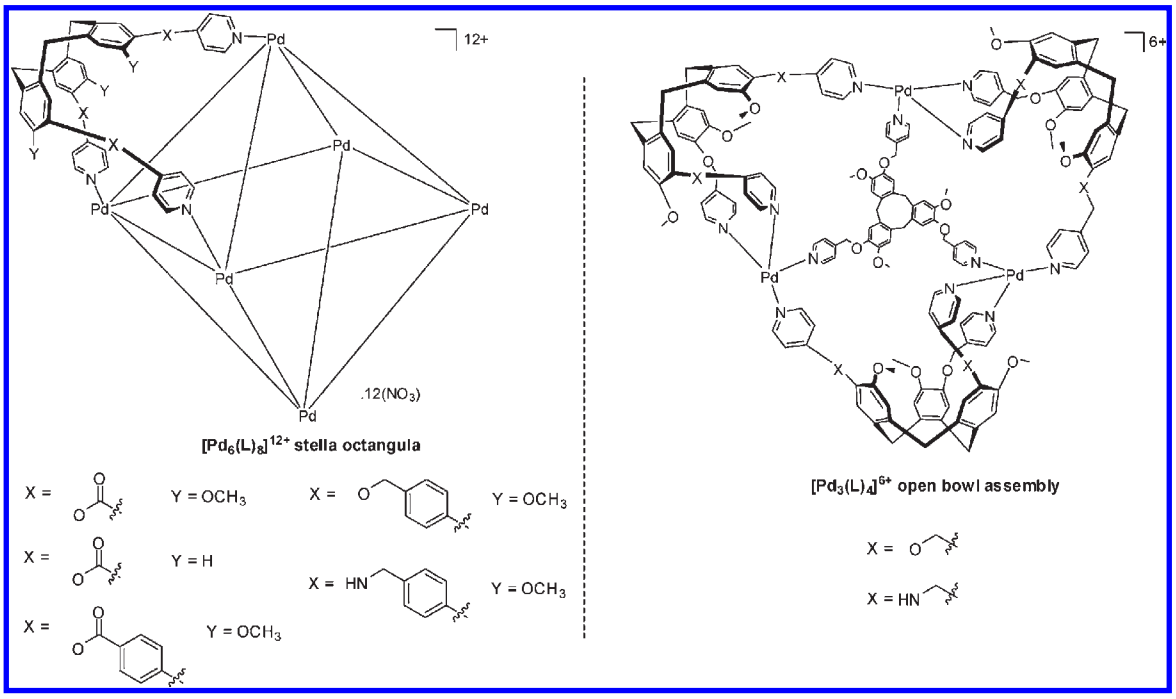

acetonitrile molecule directed into the hydrophobic cavity of the host and an additional weak C−H···O interaction (C···O distance = 3.45 Å) with one of the ester oxygen atoms of **5**. An additional acetonitrile also forms a weak C−H···O interaction (C···O distance 3.39 Å) with an ester oxygen atom. The crystal lattice has a complicated packing motif dominated by edge-to-face π-stacking interactions and face-to-face $\pi-\pi$ stacking interactions, the latter between phenyl−pyridyl arms of neighboring ligands at ring centroid separations of ca. 3.79 Å.

Metallo-Supramolecular Assemblies with Pd(II). For each of the ligands **2**−**7**, a 4:3 mixture of the ligand and $Pd(NO_3)_2$ in DMSO or d_6-DMSO was studied by electrospray ionization mass spectrometry (ESI-MS) and diffusion-ordered (DOSY) ^{1}H NMR spectroscopy. With the exception of ligands **3** and **4**, which form an open-bowl assembly discussed in detail later in the text, these solution studies demonstrated that the $[Pd_6L_8]^{12+}$ stella octangula is the dominant self-assembly product between Pd(II) and these types of ligands, Scheme 3. The complex $[Pd_6(\mathbf{7})_8]^{12+}$ is not stable in solution, as the ligand degrades when allowed to stand in solution in the presence of the metal cation.

ESI-MS provides excellent evidence that the self-assembly of a $[Pd_6(\mathbf{L})_8]^{12+}$ stella octangula cage occurs in solution for ligand **2** and all of the longer-arm ligands **5**−**7**. The electrospray mass spectrum of a DMSO solution of **2** with $Pd(NO_3)_2$ shows peaks at m/z 2087.6 and 1550.7, which are assigned to $\{Pd_6(\mathbf{2})_8(NO_3)_9\}^{3+}$ (calcd 2088.3) and $\{Pd_6(\mathbf{2})_8(NO_3)_8\}^{4+}$ (calcd 1550.7), Figure S1 (Supporting Information). The electrospray mass spectrum of the complex of **5** with $Pd(NO_3)_2$ and shows a series of peaks at m/z 2187.7, 1737.8, and 1437.6 which can be assigned to $\{Pd_6(\mathbf{5})_8(NO_3)_{(12-x)}\}^{x+}$ (x = 4−6), all arising from the octahedral core but with different numbers of anions, Figure 4. Likewise, a solution of **6** and $Pd(NO_3)_2$ shows a series of peaks at m/z 2826.2, 2103.6, 1670.5, and 1382.1 corresponding to $\{Pd_6(\mathbf{6})_8(NO_3)_{(12-x)}\}^{x+}$ (x = 3−6), Figure S2 (Supporting Information). Freshly prepared solutions of ligand **7** with $Pd(NO_3)_2$ show peaks at m/z 2816.9, 2096.7, 1664.8, and 1377.1 corresponding to $\{Pd_6(\mathbf{7})_8(NO_3)_{(12-x)}\}^{x+}$ (x = 3−6), indicating that the amine-linked derivative **7** also forms the stella octangula assembly in solution, Figure S3 (Supporting Information).

The ^{1}H NMR spectra of 4:3 mixtures of the ligands **2**, **5**, and **6** with $Pd(NO_3)_2$ in d_6-DMSO are broad and show coordination-induced shifts compared to the spectra of the free ligands. In each case, the spectra show only one set of ligand arm environments, indicating that the complexes formed retain the C_3 symmetry of the ligands. DOSY has been used to further investigate the complexes formed. DOSY has become a valuable tool for characterizing large supramolecular assemblies in solution, allowing the relative size of a molecule to be estimated from a comparison of experimental diffusion rates.[27] DOSY NMR studies of a 4:3 mixture of **2** and $Pd(NO_3)_2$ in d_6-DMSO showed a band for the major solution component with a diffusion coefficient of 0.642×10^{-10} m^2 s^{-1}. A diffusion coefficient of 1.256×10^{-10} m^2 s^{-1} was obtained for a d_6-DMSO solution of ligand **2** alone, giving a $D_{complex}/D_{ligand}$ ratio of 0.51. Although this is larger than the ratio of 0.43 observed for $[Pd_6(\mathbf{1})_8](NO_3)_{12}$,[12] it is significantly smaller than the ratio of 0.68 observed for the previously studied $[Ag_4L_4]^{4+}$ coordination cage with a

(27) For example: (a) Kamiya, N.; Tominaga, M.; Sato, S.; Fujita, M. *J. Am. Chem. Soc.* **2007**, *129*, 3816–3817. (b) Allouche, L.; Marquis, A.; Lehn, J.-M. *Chem.—Eur. J.* **2006**, *12*, 7520–7525. (c) Evan-Salem, T.; Baruch, I.; Avram, L.; Cohen, Y.; Palmer, L. C.; Rebek, J., Jr. *Proc. Natl. Acad. Sci.* **2006**, *103*, 12296–12300. (d) Megyes, T.; Jude, H.; Grosz, T.; Bako, I.; Radnai, T.; Tarkanyi, G.; Palinkas, G.; Stang, P. J. *J. Am. Chem. Soc.* **2005**, *127*, 10731–10738. (e) Tidmarch, I. S.; Taylor, B. F.; Hardie, M. J.; Russo, L.; Clegg, W.; Ward, M. D. *New J. Chem.* **2009**, *33*, 366–375.

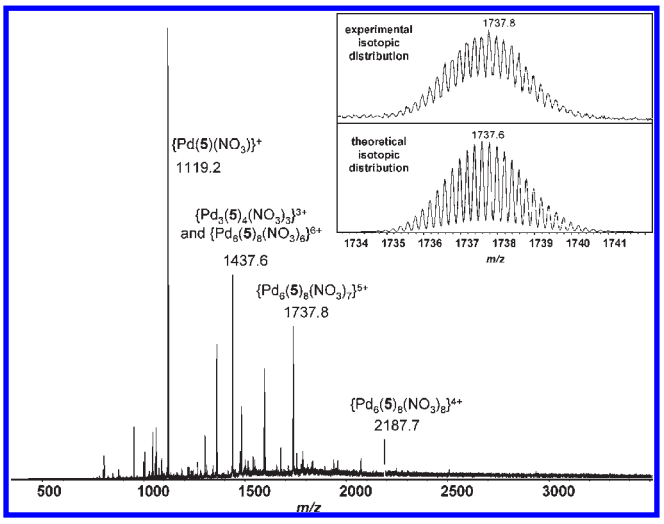

Figure 4. Electrospray mass spectrum of **5** and $Pd(NO_3)_2$ in DMSO. Inset: Theoretical and experimental isotopic distribution patterns for the $\{Pd_6(\mathbf{5})_8(NO_3)_7\}^{5+}$ peak.

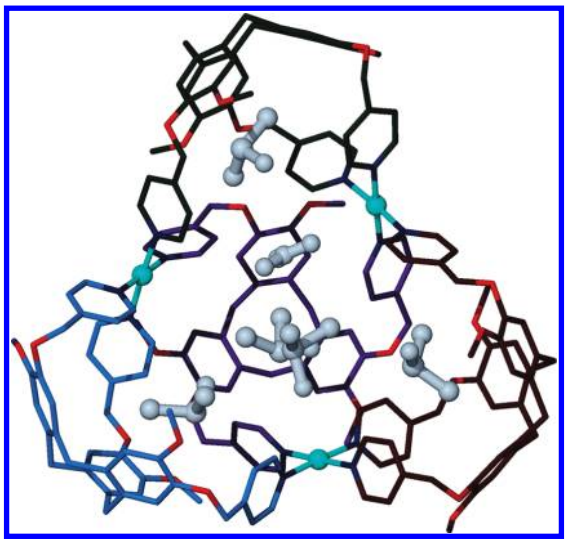

Figure 5. Detail from the crystal structure of $[Pd_3(\mathbf{3})_4](NO_3)_6 \cdot n(DMSO) \cdot m(H_2O)$. Each ligand **3** is shown in a different color, and guest NO_3^- and DMSO molecules inside the superbowl are shown as ball-and-stick.

related aminocyclotriguaiacylene-based ligand[9] and is consistent with a very large species being present in solution. Assuming that the solution species is approximately spherical, a hydrodynamic radius of 16.8 Å can be estimated using a Stokes−Einstein relationship, which is consistent with the crystal structure of $[Pd_6(\mathbf{1})_8]^{12+}$ (diameter of ca. 30 Å).

DOSY NMR studies of a 4:3 mixture of **5** and $Pd(NO_3)_2$ in d_6-DMSO showed a band for the major solution component with a diffusion coefficient of 0.477×10^{-10} m^2 s^{-1}. A diffusion coefficient of 1.032×10^{-10} m^2 s^{-1} was obtained for a d_6-DMSO solution of ligand **5** alone, giving a $D_{complex}/D_{ligand}$ ratio of 0.46. This is in good agreement with the ratio of 0.43 observed for $[Pd_6(\mathbf{1})_8]^{12+}$. The hydrodynamic radius of $[Pd_6(\mathbf{5})_8]^{12+}$ is estimated to be around 22.6 Å, somewhat larger than the hydrodynamic radius of 19.4 Å observed for $[Pd_6(\mathbf{1})_8]^{12+}$ in solution,[12] as would be expected for the larger ligand. Likewise, a 4:3 mixture of **6** and $Pd(NO_3)_2$ in d_6-DMSO showed a band with a diffusion coefficient of 0.4095×10^{-10} m^2 s^{-1}, and a solution of the ligand by itself had a diffusion coefficient of 1.112×10^{-10} m^2 s^{-1}. The $D_{complex}/D_{ligand}$ ratio of 0.37 is slightly less than that observed for the other complexes. This is likely to be due to a greater error margin in D in this case due to broadened resonance and resonance overlap observed for this system. The hydrodynamic radius of $[Pd_6(\mathbf{6})_8]^{12+}$ is estimated to be around 26.3 Å. Solutions of ligand **7** and $Pd(NO_3)_2$ were not investigated due to the instability of, and difficulties in purifying, the ligand.

In all cases, crystal growth was attempted by the diffusion of acetone vapors into the DMSO solutions. Crystalline products were isolated with ligands **2**, **5**, and **6**. These crystals were highly solvated, and X-ray data collected using rotating anode and synchrotron X-ray sources were too weak to allow for structure determinations. This is likely to be due to inherent disorder in the crystals and the subsequent lack of high-angle X-ray data. The unit cell parameters for crystals isolated from a solution of **5** and $Pd(NO_3)_2$ were F-centered cubic with $a = 51.56$ Å and $V \sim 137\,000$ Å^3. As would be expected given the larger size of the ligand, this is a much larger unit cell volume than was seen for the tetragonal crystals of $[Pd_6(\mathbf{1})_8] \cdot 12(NO_3) \cdot n(DMSO)$ where $V \sim 33\,400$ Å^3.[12]

Both ligands with relatively flexible linker groups and 4-pyridyl arms did not form the $[Pd_6L_8]^{12+}$ stella octangula assembly. Ligand **3** contains ether-linked 4-pyridyl arms and is thus more flexible than the ester-linked ligands **1** and **2**. A solution containing a mixture of **3** and $Pd(NO_3)_2$ in DMSO gave small single crystals of composition $[Pd_3(\mathbf{3})_4](NO_3)_6 \cdot n(DMSO) \cdot m(H_2O)$ upon slow diffusion of acetone vapor. The single-crystal X-ray structure was determined from data collected using synchrotron radiation and reveals a $[Pd_3(\mathbf{3})_4](NO_3)_6$ assembly which resembles an open superbowl, Scheme 3 and Figure 5.

There is one $[Pd_3(\mathbf{3})_4]^{6+}$ assembly in the asymmetric unit of the crystal structure along with counteranions and solvent. The $[Pd_3(\mathbf{3})_4]^{6+}$ assembly displays approximately C_3 (noncrystallographic) molecular symmetry, and there are two types of ligand binding modes observed. The three Pd centers are arranged in a triangle, each with square planar N_4 coordination, and Pd−N distances range from 1.973(15) to 2.054(11) Å. The central ligand forms the bottom of the bowl and bridges all three Pd centers. The other three ligands form the sides of the bowl, and each binds to only two Pd centers, with two pyridyl arms binding to the same Pd center. This binding mode is only possible due to the additional flexibility of **3** arising from the ether linkages and leads to conformation of the ligands within $[Pd_3(\mathbf{3})_4]^{6+}$ differing significantly from the conformation of ligand **1** within $[Pd_6(\mathbf{1})_8]^{12+}$, and indeed from the conformations seen in the two crystalline phases of **3** reported above. The $C_{phenyl}-O-CH_2-C_{pyridyl}$ torsion angles seen for ligand **1** in the stella octangula and for ligand **3** in both phases **3a** and **3b** are actually quite similar. Phase **3a** has torsion angles −174.0, +161.9, and +171.3°, and phase **3b** has −169.7, +167.7, and +179.6°, while in the stella octangula the two crystallographically independent ligands give angles of −172.6, +167.3, −177.9°, +174.4, +169.1, and +174°.[12] The corresponding torsion angles for ligand **3** with

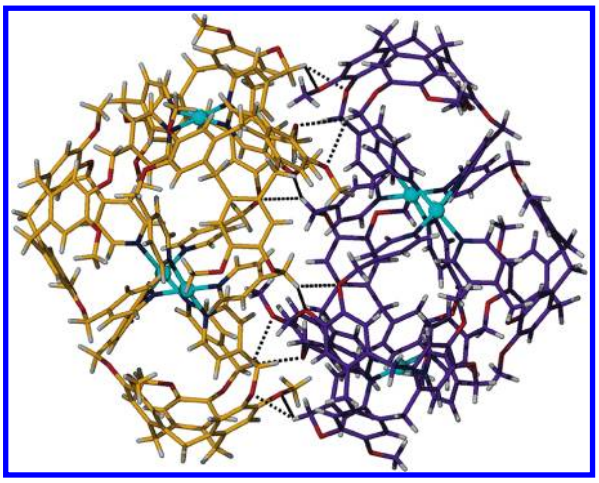

Figure 6. Detail from the crystal structure of $[Pd_3(\mathbf{3})_4](NO_3)_6 \cdot n(DMSO) \cdot m(H_2O)$, showing two of the $[Pd_3(\mathbf{3})_4]^{6+}$ superbowls hydrogen-bonding together in the solid state.

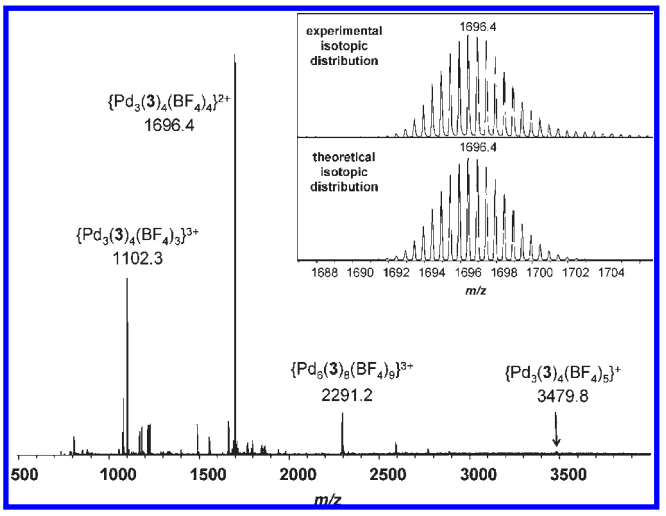

Figure 7. Electrospray mass spectrum of **3** and $[Pd(MeCN)_4](BF_4)_2$ in DMSO. Inset: Theoretical and experimental isotopic distribution patterns for the $\{Pd_3(\mathbf{3})_4(BF_4)_4\}^{2+}$ peak.

$[Pd_3(\mathbf{3})_4]^{6+}$ are quite different at +81.0, +87.2, and +87.8° for the central ligand and, for example, +70.5, +81.9, and −116.7° for one of the ligands at the side of the bowl. The Pd···Pd distances within the open-bowl assembly are 9.742, 10.144, and 10.424 Å and are significantly shorter than the Pd···Pd distances of ca. 16.6 Å in the octahedral assembly $[Pd_6(\mathbf{1})_8]^{12+}$. The depth of the bowl is 14.5 Å, as defined by the distance between the OCH_3 groups of the upper rim of the bowl and the $-(CH_2)_3-$ plane of the central ligand.

Overall, the $[Pd_3(\mathbf{3})_4]^{6+}$ assembly is a molecular host for five molecules of DMSO, Figure 5. Four of these DMSO guest molecules form host−guest interactions, each with an individual ligand, in which the hydrophobic methyl group is directed into the molecule cavity. Distances between the methyl carbon atom of the guest and the lower rim $-(CH_2)_3-$ plane of the host ligand range from 3.83 to 4.15 Å. The fifth DMSO forms a weak axial interaction with one of the Pd centers (Pd−O 3.173 Å).

In the solid state, the $[Pd_3(\mathbf{3})_4]^{6+}$ bowls dimerize through C−H···O interactions with C···O distances in the range 3.11−3.31 Å, Figure 6. Each $[Pd_3(\mathbf{3})_4]^{6+}$ bowl is homochiral, but the two bowls of the dimer have opposite chiralities. The six Pd positions within the $\{[Pd_3(\mathbf{3})_4]\}_2$ dimer form a distorted octahedron with significant elongation along one axis and the ligands positioned above each octahedral face. Hence, the hydrogen-bonded dimer is akin to a stella octangula with an oblate distortion, and its two halves are held together by weak interactions. Its long axis measures 2.7 nm, taken from the center of the C positions within the opposite lower rim $-(CH_2)_3-$ groups, which is marginally shorter than the equivalent distance of 3 nm in $[Pd_6(\mathbf{1})_8]^{12+}$.

The ^{1}H NMR spectrum of a 3:4 mixture of $Pd(NO_3)_2$ and **3** in d_6-DMSO is complicated, and it has not proved possible to specifically assign the ^{1}H signals, Figure S9 (Supporting Information). However, there is one major species, and it is notable that it does not show the C_3 symmetry of the ligand. This is consistent with the four pyridyl arm environments observed in the crystal structure of $[Pd_3(\mathbf{3})_4]^{6+}$. There was no significant change in the ^{1}H NMR spectrum upon heating the sample to 50 °C, which is consistent with the existence of a single major species in solution. DOSY NMR studies of a 4:3 mixture of ligand **3** and $Pd(NO_3)_2$ in d_6-DMSO showed a band for a major solution component with a diffusion coefficient of 0.711×10^{-10} m^2 s^{-1}. A diffusion coefficient of 1.320×10^{-10} m^2 s^{-1} was obtained for a d_6-DMSO solution of ligand **3** alone, giving a $D_{complex}/D_{ligand}$ ratio of 0.54. The appearance of the double-quantum filtered correlation spectroscopy, nuclear Overhauser effect spectrometry, and rotating-frame Overhauser enhancement spectroscopy (ROESY) spectra and 1D nuclear Overhauser effect experiments are also consistent with a single solution species.

ESI-MS gives evidence of the $[Pd_3(\mathbf{3})_4]^{6+}$ assembly existing in solution with a peak at m/z 1646.9 corresponding to $\{Pd_3(\mathbf{3})_4(NO_3)_4\}^{2+}$ (calcd 1647.4), Figure S4 (Supporting Information). However, there are also intense peaks at m/z 1530.5 and 849.2, corresponding to the mononuclear species $\{Pd(\mathbf{3})(NO_3)\}^+$ and $\{Pd(\mathbf{3})_2(NO_3)\}^+$ and a variety of other higher species including $Pd_2(\mathbf{3})_2$, $Pd_2(\mathbf{3})_3$, $Pd_3(\mathbf{3})_3$, and $Pd_4(\mathbf{3})_4$ fragments. This indicates that a mixture of species is present in the spectrometer in the gas phase. The largest mass fragment was at m/z 2216.2, which corresponds to the species $\{Pd_6(\mathbf{3})_8(NO_3)_9\}^{3+}$ (calcd 2217.5). This may indicate that a small amount of the octahedral cage exists in solution or that the hydrogen-bonded dimer of $[Pd_3(\mathbf{3})_4]^{6+}$ bowls observed in the solid state also forms in solution or within the mass spectrometer. The ESI-MS of a 3:4 solution of $[Pd(MeCN)_4](BF_4)_2$ and **3** in DMSO provides further strong evidence for the formation of the $[Pd_3(\mathbf{3})_4]^{6+}$ assembly in solution, Figure 7. Here, the spectrum shows strong peaks at m/z 1696.4 corresponding to a $\{Pd_3(\mathbf{3})_4(BF_4)_4\}^{2+}$ (calcd 1696.9) and at m/z 1102.3 corresponding to $\{Pd_3(\mathbf{3})_4(BF_4)_3\}^{3+}$ (calcd 1102.3), as well as weak peaks at m/z 3479.8 for $\{Pd_3(\mathbf{3})_4(BF_4)_5\}^+$ (calcd 3480.9) and m/z 2291.2 for the larger species $\{Pd_6(\mathbf{3})_8(BF_4)_9\}^{3+}$ (calcd 2291.6).

Tris(4-pyridylmethylamino)cyclotriguaiacylene **4** also has a flexible linker group between the host core and 4-pyridyl binding group and behaves similarly to **3** when reacted with $Pd(NO_3)_2$. As for $[Pd_3(\mathbf{3})_4]^{6+}$, the ^{1}H NMR spectrum of a 3:4 mixture of $Pd(NO_3)_2$ and **4** in d_6-DMSO

is of low symmetry and cannot be assigned, Figure S12 (Supporting Information). DOSY NMR studies of a 4:3 mixture of ligand **4** and $Pd(NO_3)_2$ in d_6-DMSO showed a band for a major solution component with a diffusion coefficient of 0.778×10^{-10} m^2 s^{-1}. A diffusion coefficient of 1.332×10^{-10} m^2 s^{-1} was obtained for a d_6-DMSO solution of ligand **4** alone, giving a $D_{complex}/D_{ligand}$ ratio of 0.58. This ratio is very similar to that observed for $[Pd_3(\mathbf{3})_4]^{6+}$. ESI-MS gives clear evidence of the formation of a $[Pd_3(\mathbf{4})_4]^{6+}$ molecular bowl. The electrospray mass spectrum of a DMSO solution of **4** with $[Pd(MeCN)_4](BF_4)_2$ in a 4:3 ratio was recorded. The major peaks in the spectrum were a +2 peak at m/z 1691.0 corresponding to a $\{Pd_3(\mathbf{4})_4(BF_4)_4\}^{2+}$ species (calcd 1690.5) and a +3 peak at m/z 1098.4 corresponding to $\{Pd_3(\mathbf{4})_4(BF_4)_3\}^{3+}$ (calcd 1098.0), Figure S5 (Supporting Information).

Conclusion

$[Pd_6L_8]^{12+}$ metallo-supramolecular assemblies with a stella octangula structure can be constructed using a number of different CTG-based ligands with 4-pyridyl donor groups. The overall size of the assembly and the size of the windows on its exterior surface can therefore be manipulated to provide a family of potential superhosts. Tris(4-pyridylmethylamino)cyclotriguaiacylene and tris(4-pyridylmethylamino) cyclotriguaiacylene were found to be an exception to this, and their more flexible ether and methyl-amine linkages allow a different binding mode to the metal, and a $[Pd_3L_4]^{6+}$ open bowl is formed. In any event, dimerization of the open bowls through weak hydrogen bonding gives an overall assembly akin to the stella octangula, at least in the solid state.

Experimental Section

Cyclotriguaiacylene,[25] cyclotriphenolene,[24] 3,8,13-triamino-2,7,12-trimethoxy-10,15-dihydro-5*H*-tribenzo[*a*,*d*,*g*]cyclononene hydrochloride (aCTG.3HCl),[26] and ligand tris(4-pyridylmethylamino)cyclotriguaiacylene, **4**,[9] were prepared according to literature methods. Electrospray mass spectra were collected at the University of Huddersfield and were measured on a Bruker MicroTOF-Q instrument in the positive ion mode. Samples of the complexes were prepared at concentrations of ca. 5 mM in DMSO and analyzed by direct infusion using a Cole Parmer syringe pump at a flow rate of 3 mL/min. Spectra were acquired over an m/z range of 50−4000; several scans were averaged to provide the final spectrum. The charge of each species (n^+) was confirmed by the spacing between the isotope components, which were $1/n$ mass units. Unless otherwise stated, reagents were obtained from commercial sources and used as received. Elemental analyses were performed by the School of Chemistry's service at the University of Leeds.

DOSY NMR Measurements. DOSY NMR measurements were measured in d_6-DMSO on a Varian Inova 500 MHz spectrometer operating under regulated temperature conditions (20 °C), with a 5 mm probe. The pulse sequence employed was a bipolar pulse pair simulated echo operating in the ONESHOT experiment. Additional parameters: number of different gradient levels, 15; gradient stabilization delay, 0.002 s; gradient length, 0.004 s; diffusion delay, 0.06 s; relaxation delay, 10 s; Kappa (unbalancing factor), 0.2. Spectra were recorded for 4 mM solutions of the ligand with added $Pd(NO_3)_2 \cdot 2H_2O$ (3:4 metal/ligand ratio). Hydrodynamic radii were estimated using a Stokes−Einstein relationship.

Synthesis. Preparation of 4-(4-Pyridyl)benzoic Acid. Prepared with minor modifications to literature methods.[28] $Pd(PPh_3)_4$ (0.53 g, 0.59 mmol) was added to a degassed solution of 4-carboxybenzene boronic acid (1.458 g, 8.786 mmol) and 4-bromopyridine hydrochloride (1.708 g, 8.783 mmol) in a 0.4 M Na_2CO_3 solution (45 mL) and acetonitrile (45 mL). The mixture was heated at 90 °C under N_2 for 16 h. The hot suspension was filtered. The filtrate was acidified with 1 M HCl and the volume reduced by half in vacuo. The white solid was collected by filtration to give 4-(4-pyridyl)benzoic acid as the hydrochloride salt (1.86 g, 90%). ^{1}H NMR (500 MHz, d_6-DMSO): δ 9.00 (2H, d, pyridyl H^2, J = 6.5 Hz), 8.40 (2H, d, pyridyl H^3, J = 6.5 Hz), 8.14 ppm (4H, m, phenyl H^2, H^3). ^{13}C NMR (75 MHz, d_6-DMSO): δ 167.0, 153.5, 144.0, 139.1, 133.3, 130.6, 128.5, 124.3 ppm. Elem anal. calcd (%) for $C_{12}H_9NO_2$·(HCl): C, 61.16; H, 4.27; N, 5.94. Found: C, 60.85; H, 4.30; N, 5.95.

Preparation of 4-(4-Pyridyl)benzoyl Chloride Hydrochloride. 4-(4-Pyridyl)benzoic acid hydrochloride (1.83 g, 7.77 mmol) was refluxed under N_2 in thionyl chloride (10 mL) containing a few drops of DMF for 24 h. The thionyl chloride was removed in vacuo and the off-white solid washed with diethyl ether to give 4-(4-pyridyl)benzoyl chloride hydrochloride in quantitative yield. ^{1}H NMR (500 MHz, d_6-DMSO): δ 9.04 (2H, d, pyridyl H^2, J = 6.5 Hz), 8.49 (2H, d, pyridyl H^3, J = 6.5 Hz), 8.16 ppm (4H, m, phenyl H^2, H^3). Elem anal. calcd (%) for $C_{12}H_8NOCl$·(HCl): C, 56.72; H, 3.57; N, 5.51; Cl, 27.9. Found: C, 55.00; H, 3.55; N, 5.25; Cl, 28.0.

Preparation of 4-[4-(Hydroxymethyl)phenyl]pyridine. A solution of $NaBH_4$ (190 mg, 5 mmol) in NaOH (0.2 M, 1.5 mL) was added dropwise to a solution of 4-(4-pyridyl)benzaldehyde (837 mg, 4.57 mmol) in MeOH (10 mL) at 0 °C and the mixture stirred for 2 h at room temperature. Aqueous Na_2CO_3 solution (0.4 M, 5 mL) was added and the mixture extracted with CH_2Cl_2 (3 × 50 mL). The combined organic layers were washed twice with water and dried over $MgSO_4$, and the solvent was evaporated. The crude product was purified by column chromatography (silica, 0−10% MeOH in CH_2Cl_2) to give 4-[4-(hydroxymethyl)phenyl]pyridine as an off-white powder (608 mg, 72%). ^{1}H NMR (500 MHz, $CDCl_3$): δ 8.65 (2H, d, pyridyl H^2, J = 6.0 Hz), 7.65 (2H, d, phenyl H^3, J = 8.1 Hz), 7.48−7.30 (4H, m, phenyl H^2 and pyridyl H^3), 4.78 ppm (2H, s, CH_2). ^{13}C NMR (75 MHz, $CDCl_3$): δ 150.6, 148.5, 142.5, 137.7, 128.0, 127.6, 122.0, 65.1 ppm. Elem anal. calcd (%) for $C_{12}H_{11}NO(H_2O)_{0.1}$: C, 77.06; H, 6.04; N, 7.49. Found: C, 76.80; H, 5.95; N, 7.15. All other data matched those previously reported.[29]

Preparation of 4-[4-(Chloromethyl)phenyl]pyridine Hydrochloride. Thionyl chloride (1 mL, 14 mmol, excess) was added to a solution of 4-[4-(hydroxymethyl)phenyl]pyridine (608 mg, 3.28 mmol) in dry $CHCl_3$ (50 mL) at room temperature. The mixture was stirred overnight, and the solvent removed in vacuo. The crude product was dried in vacuo for 2 h and used without further purification.

Preparation of Tris(isonicotinoyl)cyclotriphenolene (2). Cyclotriphenolene (98 mg, 0.31 mmol) was dissolved in dry THF (30 mL) under a N_2 atmosphere and cooled to −78 °C in a dry ice/acetone bath. Triethylamine (0.55 mL) was added to the reaction, which was stirred for 30 min. Isonicotinoyl chloride hydrochloride (192 mg, 1.08 mmol) was added to the solution, which was stirred at −78 °C for 1 h, and then refluxed for 2 days. The solution was taken to dryness in vacuo and the residue triturated with ethanol to give **2** as a white solid (102 mg 52%). Mp 248−241 °C. ^{1}H NMR (500 MHz, $CDCl_3$): δ 8.78 (6H, d,

(28) Gong, Y.; Pauls, H. W. *Synlett*. **2000**, 829–831.

(29) Blanco, V.; Abella, D.; Pia, E.; Platas-Iglesias, C.; Peinador, C.; Quintela, J. M. *Inorg. Chem*. **2009**, *48*, 4098–4197.

(30) (a) Kamiya, N.; Tominaga, M.; Sato, S.; Fujita, M. *J. Am. Chem. Soc*. **2007**, *129*, 3816–3817. (b) Allouche, L.; Marquis, A.; Lehn, J.-M. *Chem.—Eur. J*. **2006**, *12*, 7520–7525.

pyridyl H^2, J = 5.6 Hz), 7.91 (6H, d, pyridyl H^3, J = 5.6 Hz), 7.38 (3H, d, aryl CH), 7.19 (3H, dd, aryl CH), 6.95 (3H, dd, aryl CH), 4.85 (3H, d, CH_2, J = 13.7 Hz), 3.76 ppm (3H, d, CH_2, J = 13.7 Hz). ^{13}C NMR (75 MHz, $CDCl_3$): δ 162.7, 149.8, 148.3, 139.7, 135.9, 135.8, 130.4, 122.2, 121.6, 119.2, 35.7 ppm. HR MS (ES^+): m/z 634.1969 (MH^+). Calcd for $C_{39}H_{28}N_3O_6$ 634.1973. Elem anal. calcd (%) for $C_{39}H_{27}N_3O_6(H_2O)$: C, 71.88; H, 4.49; N, 6.45. Found: C, 72.35; H, 4.85; N, 6.25.

Preparation of Tris(4-pyridylmethyl)cyclotriguaiacylene (3). NaH (60% dispersion in mineral oil, 200 mg, 4.92 mmol) was added in small portions to a solution of CTG (200 mg, 0.490 mmol) in dry DMF (7 mL) and the mixture stirred for 30 min under N_2. A solution of 4-bromomethylpyridine (2.45 mmol) in dichloromethane (30 mL) was added by syringe and the mixture stirred at room temperature for 48 h. Water (100 mL) and CH_2Cl_2 (100 mL) were added and the aqueous layer washed with CH_2Cl_2 (2 × 100 mL). The combined organic layers were washed with water (5 × 100 mL), dried ($MgSO_4$), and evaporated in vacuo. The residue was purified by column chromatography (silica, 5% MeOH in CH_2Cl_2) to afford **3** as an off-white powder (262 mg, 79%). [4-Bromomethylpyridine was freshly prepared before use by the following method: A saturated aqueous Na_2CO_3 solution was added dropwise to a stirred solution of 4-bromomethylpyridine·HBr (620 mg, 2.45 mmol) in distilled water (20 mL) at 0 °C to reach ~pH 7. Then, 4-bromomethylpyridine was extracted with CH_2Cl_2 (30 mL), dried over $MgSO_4$, and filtered. The filtrate was used without further purification.] Mp 138−143 °C. ^{1}H NMR (500 MHz, $CDCl_3$): δ 8.60 (6H, d, pyridyl H^2, J = 6 Hz), 7.34 (6H, d, pyridyl H^4, J = 6 Hz), 6.78 (3H, s, aryl CH), 6.66 (3H, s, aryl CH), 5.11 (6H, s, CH_2−O), 4.70 (3H, d, CTG CH_2, J = 13.8 Hz), 3.71 (9H, s, CH_3) 3.46 ppm (3H, d, CTG CH_2, J = 13.8 Hz). ^{13}C NMR (75 MHz, $CDCl_3$): δ 150.0, 148.5, 146.7, 146.5, 133.2, 131.6, 121.2, 116.3, 113.7, 70.0, 56.1, 36.5 ppm. HR MS (ES^+): m/z 682.2932 (MH^+). Calcd for $C_{42}H_{40}N_3O_6$, 682.2912. Elem anal. calcd (%) for $C_{42}H_{39}N_3O_6(H_2O)_{0.5}$: C, 73.03; H, 5.84; N, 6.08. Found: C, 72.95; H, 6.05; N, 5.75.

Preparation of Tris[4-(4-pyridyl)benzoyl]cyclotriguaiacylene (5). Cyclotriguaiacylene (153 mg, 0.375 mmol) was dissolved in dry THF (30 mL) under a N_2 atmosphere and cooled to −78 °C in a dry ice/acetone bath. Triethylamine (0.65 mL) was added to the reaction, which was stirred for 30 min. 4-(4-Pyridyl)benzoyl chloride hydrochloride (320 mg, 1.26 mmol) was added to the solution, which was stirred at −78 °C for 1 h and then at room temperature for 2 days. A further portion of 4-(4-pyridyl)-benzoyl chloride hydrochloride (320 mg, 1.26 mmol) was added and the mixture stirred for a further 2 days. The solution was taken to dryness in vacuo and the residue triturated with ethanol to give **5** as a white solid (287 mg, 80%). Mp 255−260 °C (decomposition). ^{1}H NMR (500 MHz, $CDCl_3$): δ 8.73 (6H, d, pyridyl H^2, J = 5.9 Hz), 8.31 (6H, d, phenyl H^3, J = 8.4 Hz), 7.77 (6H, d, phenyl H^2, J = 8.4 Hz), 7.56 (6H, d, pyridyl H^3, J = 5.9 Hz), 7.20 (3H, s, aryl CH), 6.98 (3H, s, aryl CH), 4.86 (3H, d, CTG CH_2, J = 13.8 Hz), 3.82 (9H, s, CH_3), 3.71 ppm (3H, d, CTG CH_2, J = 13.8 Hz). ^{13}C NMR (75 MHz, $CDCl_3$): δ 164.2, 150.5, 150.0, 147.1, 143.1, 138.6, 138.1, 131.6, 131.1, 130.0, 127.2, 124.1, 121.7, 114.3, 56.3, 36.6 ppm. HR MS (ES^+): m/z 952.3232 (MH^+). Calcd for $C_{60}H_{46}N_3O_9$, 952.3229. Elem anal. calcd (%) for $C_{60}H_{45}N_3O_9(H_2O)$: C, 74.29; H, 4.88; N, 4.33. Found: C, 74.45; H, 4.75; N, 4.20.

Preparation of Tris{4-(4-pyridyl)benzyl}cyclotriguaiacylene (6). NaH (60% dispersion in mineral oil, 470 mg, 11.8 mmol) was added in small portions to a solution of CTG (236 mg, 0.578 mmol) in dry DMF (7 mL) and the mixture stirred for 30 min. Solid 4-[4-(chloromethyl)phenyl]pyridine hydrochloride (694 mg, 2.89 mmol) was added and the mixture stirred at room temperature for 48 h. Water (100 mL) and CH_2Cl_2 (100 mL) were added, and the aqueous layer washed with CH_2Cl_2 (2 × 100 mL). The combined organic layers were washed with water (5 × 100 mL) and dried ($MgSO_4$) and the solvent removed in vacuo. The residue was purified by column chromatography (silica, 0−5% MeOH in CH_2Cl_2) to afford **6** as a white powder (357 mg, 68%). Mp 143−145 °C. ^{1}H NMR (500 MHz, $CDCl_3$): δ 8.66 (6H, d, pyridyl H^2, J = 5.1 Hz), 7.64 (6H, d, phenyl H^3, J = 8.1 Hz), 7.48−7.55 (12H, m, phenyl H^2 and pyridyl H^3), 6.86 (3H, s, aryl CH), 6.71 (3H, s, aryl CH), 5.16 (6H, m, CH_2−O), 4.72 (3H, d, CTG CH_2, J = 13.9 Hz), 3.67 (9H, s, CH_3), 3.49 ppm (3H, d, CTG CH_2, J = 13.9 Hz). ^{13}C NMR (75 MHz, $CDCl_3$): δ 150.4, 148.5, 147.8, 147.0, 138.6, 137.7, 132.8, 131.8, 127.7, 127.2, 121.5, 116.2, 113.9, 71.1, 56.2, 36.5 ppm. HR MS (ES^+): m/z 910.3824 (MH^+). Calcd for $C_{60}H_{52}N_3O_6$, 910.3851. Elem anal. calcd (%) for $C_{60}H_{51}N_3O_6(H_2O)$: C, 77.65; H, 5.76; N, 4.53. Found: C, 77.95; H, 5.75; N, 4.50.

Preparation of Tris[4-(4-pyridyl)benzylamino]cyclotriguaiacylene (7). A mixture of aCTG·3HCl (445 mg, 0.864 mmol), 4-(4-pyridyl)benzaldehyde (500 mg, 2.73 mmol), and triethylamine (1.75 mL) in ethanol (50 mL) was refluxed for 3 h to give a yellow solution. The reaction mixture was cooled to room temperature and the solvent removed in vacuo to give a bright yellow solid. This was dissolved in a 1:1 mixture of dichloromethane and ethanol (40 mL), sodium borohydride (500 mg, 13.1 mmol) was added in small portions and the reaction mixture stirred at room temperature for 72 h. The solvent was removed in vacuo and the solid taken up in dichloromethane (150 mL), the chlorinated extract washed with water (50 mL) and then dried over $MgSO_4$. The solvent was removed in vacuo and the crude product purified by column chromatography (silica, 5% MeOH in CH_2Cl_2 with a few drops of Et_3N) to give slightly impure **7** (~90% purity by NMR). Yield: 382 mg, 48%. All further attempts to purify the product were unsuccessful. HR MS (ES^+): m/z 907.4308 (MH^+). Calcd for $C_{60}H_{55}N_6O_3$, 907.4330. ^{1}H NMR (500 MHz, $CDCl_3$): δ 8.65 (6H, d, pyridyl H^2, J = 4.9 Hz), 7.61 (6H, d, phenyl H^3, J = 8.1 Hz), 7.50 (6H, d, pyridyl H^3, J = 4.9 Hz), 7.47 (6H, d, phenyl H^2, J = 8.1 Hz), 6.50 (3H, s, aryl CH), 6.47 (3H, s, aryl CH), 4.68 (3H, d, CTG CH_2, J = 13.7 Hz), 4.41 (6H, s, br, $NHCH_2$), 3.49 (9H, s, CH_3), 3.37 ppm (3H, d, CTG CH_2, J = 13.7 Hz).

Reaction of 2 with $Pd(NO_3)_2$. $Pd(NO_3)_2·2H_2O$ (5 mg, 0.019 mmol) was added to a solution of tris(isonicotinoyl)cyclotriphenolene (15 mg, 0.024 mmol) in DMSO (1.5 mL). Acetone diffusion into the solution gave heavily solvated colorless crystals of $[Pd_6(2)_8](NO_3)_{12}$, which were isolated by filtration and dried in vacuo. Yield: 14 mg. ^{1}H NMR (500 MHz, d_6-DMSO): δ 9.54 (6H, d, pyridyl H^2), 8.27 (6H, d, pyridyl H^3), 7.56 (3H, m, aryl CH), 7.39 (3H, s, br, aryl CH), 6.89 (3H, m, aryl CH), 4.85 (3H, s, br, CH_2), 3.76 ppm (3H, s, br, CH_2). IR (solid state): ν 3106 (w), 3056 (w), 3022 (w), 2916 (w), 1750 (s), 1654 (w), 1621 (w), 1586 (w), 1564 (w), 1494 (m), 1430 (m), 1343 (m), 1371 (s, NO_3^-), 1234 (s), 1186 (m), 1148 (m), 1106 (m), 1084 (w), 1057 (m), 1020 (s), 951 (m), 862 (w), 829 (w), 763 (w), 753 (w), 693 (m), 620 (w), 577 cm^{-1} (w). ES MS (DMSO solution): m/z 2087.6 $\{Pd_6(\mathbf{2})_8(NO_3)_9\}^{3+}$ (calcd 2088.3), 1550.7 $\{Pd_6(\mathbf{2})_8(NO_3)_8\}^{4+}$ (calcd 1550.7), 1434.3 $\{Pd(\mathbf{2})_2(NO_3)\}^+$ (calcd 1434.3), 1233.6 $\{Pd_3(\mathbf{2})_3(NO_3)_4\}^{2+}$ (calcd 1233.6), 801.1 $\{Pd(\mathbf{2})(NO_3)\}^+$ (calcd 801.1). The crystals of $[Pd_6(\mathbf{2})_8](NO_3)_{12}·n(DMSO)·m(H_2O)$ were highly solvated, and satisfactory microanalytical results could not be obtained.

Preparation of $[Pd_3(\mathbf{3})_4](NO_3)_6·n(DMSO)·m(H_2O)$. $Pd(NO_3)_2·2H_2O$ (12 mg, 0.045 mmol) was added to a solution of tris(4-pyridylmethyl)cyclotriguaiacylene (40 mg, 0.059 mmol) in DMSO (5 mL). Acetone diffusion into the solution gave heavily solvated colorless crystals of $[Pd_3(\mathbf{3})_4](NO_3)_6·n(DMSO)·m(H_2O)$ which were isolated by filtration and dried in vacuo (33 mg). IR (solid state): ν 3097 (w), 2983 (w), 2932 (w), 2852 (w), 1655 (w), 1609 (m), 1508 (s), 1479 (w), 1434 (m), 1397 (w), 1339 (s, NO_3^-), 1275 (m), 1257 (s), 1214 (m), 1198 (m), 1144 (m), 1086 (m), 1063 (w), 1021 (s), 994 (w), 948 (m), 928 (w), 892 (w), 848 (m), 829 (w), 813 (m), 741 (m), 705 (w), 665 (w), 647 (w), 618 (m),

Table 1. Details of Data Collections and Structure Refinements for X-Ray Structures

	2	**3a**	**3b**	**5**·3$^1/_3$MeCN·$^1/_3$H$_2$O	[Pd$_3$(**3**)$_4$](NO$_3$)$_6$
formula	$C_{39}H_{27}N_3O_6$	$C_{42}H_{39}N_3O_6$	$C_{42}H_{39}N_3O_6$	$C_{66.67}H_{55.67}N_{6.33}O_{9.33}$	$C_{184}H_{209}N_{15}O_{43.5}Pd_8S_3$
Mr	633.64	681.76	681.76	1094.84	4274.04
cryst size [mm]	0.20 × 0.18 × 0.17	0.50 × 0.15 × 0.08	0.12 × 0.10 × 0.05	0.50 × 0.40 × 0.20	0.15 × 0.10 × 0.06
cryst syst	triclinic	monoclinic	rhombohedral	trigonal	monoclinic
space group	$P\bar{1}$	$P2(1)/n$	$R\bar{3}$	$P31c$	$C2/c$
a [Å]	4.6791(4)	16.2129(19)	62.828(4)	19.3666(4)	43.49(3)
b [Å]	14.1061(10)	7.9897(9)	62.828(4)	19.3666(4)	28.10(3)
c [Å]	24.9786(18)	27.423(3)	9.8070(13)	28.7185(16)	40.83(4)
α [deg]	74.971(4)	90	90	90	90
β [deg]	88.487(4)	103.168(6)	90	90	100.545(15)
γ [deg]	80.645(4)	90	120	120	90
V [Å^3]	1570.9(2)	3458.8(7)	33525(5)	9328.2(6)	49058(79)
Z	2	4	36	6	8
ρ_{calcd} [g cm^{-3}]	1.340	1.309	1.216	1.169	1.157
μ [cm^{-1}]	0.092	0.088	0.082	0.079	0.659
θ range [deg]	0.84 to 26.00	1.34 to 31.53	1.12 to 25.00	1.21 to 25.00	3.19 to 17.75
data collected	26374	67963	157844	165090	70813
unique data, R_{int}	6142, 0.0299	11517, 0.0290	13127, 0.0928	10939, 0.0346	15312, 0.1208
obs. data [$I > 2\sigma(I)$]	4400	8317	7986	9211	9929
data/restraints/params	6142/0/433	11517/0/463	13127/0/925	10939/1/718	15312/48/1123
R_1 [obs. data]	0.0437	0.0464	0.0598	0.0763	0.1122
wR_2 [all data]	0.1312	0.1516	0.2249	0.2447	0.3267
absolute structure parameter				0.4(14)	
GOF	0.978	1.039	1.080	1.091	1.071

531 cm^{-1} (w). ES MS (DMSO solution): m/z 2216.2 {Pd$_6$(**3**)$_8$(NO$_3$)$_9$}$^{3+}$ (calcd 2216.9), 1762.4 {Pd$_2$(**3**)$_2$(NO$_3$)$_3$}$^+$ and {Pd$_4$(**3**)$_4$(NO$_3$)$_6$}$^{2+}$ (calcd 1762.3), 1646.9 {Pd$_3$(**3**)$_4$(NO$_3$)$_4$}$^{2+}$ (calcd 1646.9), 1530.5 {Pd(**3**)$_2$(NO$_3$)}$^+$ (calcd 1530.5), 1306.3 {Pd$_3$(**3**)$_3$(NO$_3$)$_4$}$^{2+}$ (calcd 1305.8), 1190.8 {Pd$_2$(**3**)$_3$(NO$_3$)$_2$}$^{2+}$ (calcd 1190.8), 849.2 {Pd(**3**)(NO$_3$)}$^+$ (calcd 849.2). Microanalytical results indicate the crystals were highly solvated. Example of elemental analysis, calcd (%) for Pd$_3$(C$_{42}$H$_{39}$N$_3$O$_6$)$_4$(NO$_3$)$_6$(C$_2$H$_6$SO)$_{12}$(H$_2$O)$_6$: C, 51.66; H, 5.42; N, 5.65; S, 8.62. Found: C, 51.60; H, 5.55; N, 5.75; S, 8.45.

Reaction of 5 with Pd(NO$_3$)$_2$. Pd(NO$_3$)$_2$·2H$_2$O (4 mg, 0.015 mmol) was added to a solution of tris[4-(4-pyridyl)benzoyl]-cyclotriguaiacylene (15 mg, 0.016 mmol) in DMSO (2 mL). Acetone diffusion into the solution gave heavily solvated colorless crystals of [Pd$_6$(**5**)$_8$](NO$_3$)$_{12}$, which were isolated by filtration and dried in vacuo (15 mg). Crystals of [Pd$_6$(**5**)$_8$](NO$_3$)$_{12}$ can also be isolated from acetone diffusion into a DMSO solution with a 3:4 metal/ligand ratio. ^{1}H NMR (500 MHz, d_6-DMSO): δ 9.46 (6H, s, br, pyridyl H^2), 8.22 (6H, s, br), 8.17 (6H, s, br), 8.10 (6H, s, br), 7.49 (3H, s, aryl CH), 7.31 (3H, s, aryl CH), 4.91(3H, s, br, CTG CH$_2$), 3.45 ppm (12H, m, CTG CH$_2$ and CH$_3$). IR (solid state): ν 3007 (w), 2918 (w), 1735 (s), 1643 (m), 1615 (s), 1508 (s), 1466 (w), 1436 (m), 1403 (m), 1329 (s, NO$_3^-$), 1266 (s), 1206 (m), 1179 (s), 1139 (m), 1092 (m), 1062 (w), 1013 (s), 951 (s), 901 (w), 871 (w), 836 (m), 767 (m), 736 (w), 704 (m), 623 (w), 567 (w), 530 (w), 510 cm^{-1} (w);. ES MS (DMSO solution): m/z 2187.7 {Pd$_6$(**5**)$_8$(NO$_3$)$_8$}$^{4+}$ (calcd 2187.5), 1737.8 {Pd$_6$(**5**)$_8$(NO$_3$)$_7$}$^{5+}$ (calcd 1737.6), 1596.4 {Pd$_2$(**5**)$_3$(NO$_3$)$_2$}$^{2+}$ and {Pd$_4$(**5**)$_6$(NO$_3$)$_4$}$^{4+}$ (calcd 1596.4), 1437.6 {Pd$_3$(**5**)$_4$(NO$_3$)$_3$}$^{3+}$ and {Pd$_6$(**5**)$_8$(NO$_3$)$_6$}$^{6+}$ (calcd 1437.6), 1361.0 {Pd$_2$(**5**)$_4$(NO$_3$)}$^{3+}$ (calcd 1360.7), 1119.2 {Pd(**5**)(NO$_3$)}$^+$ (calcd 1119.2), 1062.2 {Pd$_3$(**5**)$_4$(NO$_3$)$_2$}$^{4+}$ (calcd 1062.7). The crystals of [Pd$_6$(**5**)$_8$](NO$_3$)$_{12}$ were highly solvated. Example of elemental analysis, calcd (%) for Pd$_6$(C$_{60}$H$_{45}$N$_3$O$_9$)$_8$(NO$_3$)$_{12}$(C$_2$H$_6$SO)$_8$(H$_2$O)$_{25}$: C, 59.14; H, 4.59; N, 5.01; S, 2.54. Found: C, 59.10; H, 4.30; N, 4.70; S, 2.40; %.

Reaction of 6 with Pd(NO$_3$)$_2$. Pd(NO$_3$)$_2$·2H$_2$O (4 mg, 0.015 mmol) was added to a solution of tris{4-(4-pyridyl)benzyl}-cyclotriguaiacylene (15 mg, 0.016 mmol) in DMSO (2 mL). Acetone diffusion into the solution gave a small amount of colorless crystals. The product was not isolated in sufficient quantities for solid-state characterization. Crystals of [Pd$_6$(**6**)$_8$](NO$_3$)$_{12}$ can also be isolated from acetone diffusion into a DMSO solution with a 3:4 metal/ligand ratio. ^{1}H NMR (500 MHz, d_6-DMSO): δ 9.35 (6H, s, br), 8.16 (6H, s, br), 7.91 (6H, d), 7.53 (6H, d), 7.25 (3H, s, aryl CH), 7.17 (3H, s, aryl CH), 5.07 (3H, s, br), 4.51−4.54 (6H, m), 3.50−3.53 ppm (9H, m, CTG CH$_2$ and CH$_3$). ES MS (DMSO solution): m/z 2826.2 {Pd$_6$(**6**)$_8$(NO$_3$)$_9$}$^{3+}$ (calcd 2825.4), 2103.6 {Pd$_6$(**6**)$_8$(NO$_3$)$_8$}$^{4+}$ (calcd 2103.6), 1987.7 {Pd(**6**)$_2$(NO$_3$)}$^+$ and {Pd$_2$(**6**)$_4$(NO$_3$)$_2$}$^{2+}$ (calcd 1986.6), 1670.5 {Pd$_6$(**6**)$_8$(NO$_3$)$_7$}$^{5+}$ (calcd 1670.5), 1533.0 {Pd$_2$(**6**)$_3$(NO$_3$)$_2$}$^{2+}$ and {Pd$_4$(**6**)$_6$(NO$_3$)$_4$}$^{4+}$ (calcd 1533.5), 1382.1 {Pd$_6$(**6**)$_8$(NO$_3$)$_6$}$^{6+}$ (calcd 1381.7), 1077.3 {Pd(**6**)(NO$_3$)}$^+$ and {Pd$_2$(**6**)$_2$(NO$_3$)$_2$}$^{2+}$ (calcd 1077.3), 1002.0 {Pd$_2$(**6**)$_3$(NO$_3$)}$^{3+}$ (calcd 1001.6), 962.4 {Pd(**6**)$_2$}$^{2+}$ (calcd 962.3). Crystals were highly solvated, and satisfactory microanalysis could not be obtained.

X-Ray Crystallography. Crystals were mounted under oil on a glass fiber and X-ray diffraction data collected at 150(1) K with either Mo Kα radiation (λ = 0.71073 Å) using a Bruker Nonius X-8 diffractometer with ApexII detector and FR591 rotating anode generator, or with synchrotron radiation at STFC Daresbury laboratory station 16.2SMX (λ = 0.7977 Å). Data sets were corrected for absorption using a multiscan method, and structures were solved by direct methods using SHELXS-97[31] and refined by full-matrix least-squares on F^2 by SHELXL-97,[32] interfaced through the program X-Seed.[33] In general, all non-hydrogen atoms were refined anisotropically, and hydrogen atoms were included as invariants at geometrically estimated positions, unless specified otherwise. Details of data collections and structure refinements are given in Table 1. Crystallographic data have been deposited with the Cambridge Crystallographic Data Centre as supplementary publications CCDC 742268−742272.

Crystals of [Pd$_3$(**3**)$_4$](NO$_3$)$_6$·n(DMSO)·m(H$_2$O) were poorly diffracting, even with synchrotron radiation, and only data with $2\theta \leq 45°$ were used in the final refinement. SAME and SADI restraints were applied to the poorly ordered DMSO solvent molecules and nitrate anions to ensure a stable refinement. Hydrogen atoms were included as invariants at geometrically

(31) Sheldrick, G. M. *SHELXS-97*; University of Göttingen: Göttingen, Germany, 1990.
(32) Sheldrick, G. M. *SHELXL-97*; University of Göttingen: Göttingen, Germany, 1997.
(33) Barbour, L. J. *J. Supramol. Chem.* **2003**, *1*, 189–191.

estimated positions, aside from those of a disordered DMSO molecule and water molecules, which were excluded. Only three of the expected six anions could be located, and these were refined with isotropic displacement parameters. The SQUEEZE[34] function was applied to remove areas of diffuse electron density, which could not be modeled, which presumably accounts for the remaining anions and severely disordered solvent molecules.

(34) Spek, A.; van der Sluis, P. *Acta Crystallogr., Sect. A* **1990**, *46*, 194.

Acknowledgment. We thank the EPSRC for their financial support of this research, and thank STFC Daresbury laboratory for access to microdiffraction facilities, Ian Blakeley for performing elemental analyses, and Tanya Marinko-Covell for some mass spectrometry measurements.

Supporting Information Available: ESI-MS spectra; 1-D, DOSY, and ROESY NMR spectra; and crystallographic information files (CIF) are available. This information is available free of charge via the Internet at http://pubs.acs.org.